

# Novel MR-Safe Guidewire with Passive Iron-Platinum Alloy Nanoparticles for MR-Guided Interventions

Martin Alexander Rube<sup>1</sup>, Patricia Seifert<sup>2</sup>, Bernhard Uihlein<sup>2</sup>, Dhanapriya Kakchingtabam<sup>3</sup>, Pascal André<sup>3</sup>, and Andreas Melzer<sup>1</sup>

<sup>1</sup>Institute for Medical Science and Technology, University of Dundee, Dundee, United Kingdom, <sup>2</sup>EPflex Feinwerktechnik GmbH, Dettingen, Germany, <sup>3</sup>School of Physics and Astronomy (SUPA), University of St Andrews, St. Andrews, United Kingdom

**Purpose:** MRI-guided interventions (iMRI) are still challenging and generally limited to research centres. The largest hurdle to overcome has been the shortage of MR safe devices and in this context, guidewires (GW) appear as key devices for cardiovascular iMRI. To date few concepts, ex-vivo, animal [1, 2] and first-in-man studies [3] of MRI-compatible GWs have been published, but no MR safe GW is approved for clinical use. Reliable device tracking and visualization is essential and recently a visualization method for positive contrast imaging of passive markers has been published [4] where paramagnetic markers appear hyperintense on an almost completely dark background. This enables interactive tracking in a similar manner as active tracking using projectional images [5]. In this study a passive GW localisation method based on iron-platinum alloy nanoparticles (FePt nPs) is proposed. The FePt nPs have been developed as biocompatible strong  $T_2$  contrast agents with a large  $T_2$  relaxivity ( $r_2$ ) for biomedical applications [6].

**Materials and Methods:** A passive marker solvent consisting of in-house synthesized FePt NPs in a polymeric matrix was applied to a novel MR safe GW prototype (MRLine, EPflex) using a micropipette. The imaging properties of various FePt nP concentrations (2.5 mg / mL, 5 mg / mL, 20 mg / mL) in a polymeric matrix have been compared for marking GWs. The hydrophilic coated 0.035" GW consists of a high-strength core surrounded by bending resistant synthetic material. Six 10 mm markers, each 10  $\mu$ L FePt nPs were distributed over the tip section of the GW. MR images were obtained in a clinical 1.5 T scanner (Signa HDx 1.5 T, GE) with 8-channel body array coil. High-resolution and almost real-time imaging was conducted in plastic box, an arterial vessel replica model (L-F-S-Left-003, Elastrat) containing 0.9% saline solution and in a Thiel soft embalmed human cadaver model using fast steady-state and spoiled gradient-echo sequences. A 12 F introducer sheath (Cook Medical) was placed into the femoral vein and the GW was inserted and positioned in the Vena Cava (filled with Thiel moistening solution). Image analysis was performed in MATLAB (Mathworks) and OsiriX (Aycan). Marker sizes were measured during black marker imaging (Fig. 1a) in coronal and axial planes in slices where signal voids of the markers showed a maximum for the long axis (a) aligned with  $B_0$ .

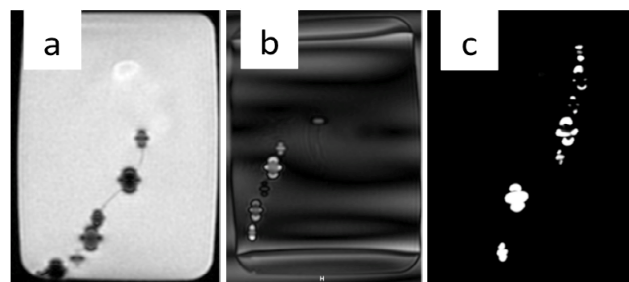


**Fig. 1 – GW prototype a) Black Marker Imaging: FSPGR TE/TR = 10 / 100 ms FA = 60° b) White Marker imaging: FIESTA TE/TR = 2.4 / 4.8 ms FA = 80° c) MIP (Axial) of FIESTA as (b)**



FePt concentration	Axis (a)	Axis (b)
2.5 mg / mL	3 – 6 mm	5 – 8 mm
5 mg / mL	4 – 8 mm	6 – 9 mm
20 mg / mL	12 – 15 mm	9 – 13 mm

**Fig. 2 - FePt Artifact Measurements (Parameters acc. Fig. 1a)**

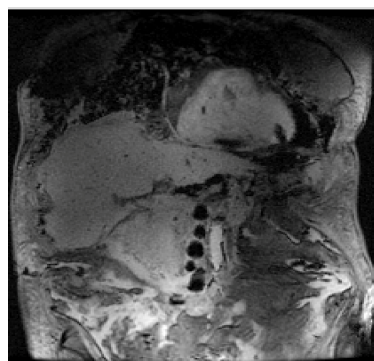


**Fig. 3 – GW in the Vena Cava of a Thiel Embalmed Human Cadaver: FSPGR TE/TR = 10 / 100 ms FA = 60°**

**Results:** The signal void sizes resulting from the different FePt nP concentrations on the GW are summarized in Fig. 2. According to the phantom experiments the GW with the 20 mg / mL FePt nPs concentration was chosen for cadaver experiments and imaging parameters were optimized for iMRI (FGRE TE/TR = 1.5 / 4.5 ms FA 40°) and anatomical cadaver imaging (FSPGR TE/TR = 1.7 / 100 ms FA 60°). GW manoeuvring into the targeted vessel segments under MR guidance was successful for both the vessel model and Thiel embalmed cadavers (2 of 2). In the cadaver experiments (Fig. 2) the markers showed ball shaped artefacts rather than the dipole - dipole artefacts as during the phantom experiments (Fig 1.). The artefact size was mainly depending on the GW orientation in respect to  $B_0$  and increasing with TE. In almost real-time MRI, the induced artefacts enabled a distinct visualization of the GW with a mean marker size of 14 mm (long axis) and 12 mm (short axis), respectively. This facilitated fast navigation to target vessel segments and was successfully evaluated by two experienced interventional radiologists assessing overall GW visibility and performance (pushability, torque and gliding properties).

**Discussion and Conclusion:** MR-guided cardiovascular interventions require visualization of catheters and GWs with respect to the vessels and anatomy of interest. The artefacts resulting from the FePt nPs have been optimised for experimental use and can be manipulated by changing the sequence parameters (mainly TE) or the FePt nP concentration. However, iMRI sequences require high framerates and

therefore a short TE. The two lower FePt concentrations were found to be useful for phantom imaging but generally hard to identify during cadaver experiments with very short TE. The passive marker solvent with 20 mg / mL FePt nPs was found most useful for localizing GWs during MR-guided interventions (up to 4 fps). The solvent with 20 mg / mL FePt nPs exhibited good-sized signal voids and allowed for a low amount of solvent on the GW without decreasing the GW performance. The phantom and Thiel cadaver experiments demonstrate that the GW prototype with FePt nP markers is well-suited for MR guided interventions and has potential for automated device tracking and slice repositioning [5]. This approach opens novel prospects for the realization of endovascular and cardiovascular iMRI that need to be explored in further studies.

## References:

- [1] Kos, S et al. Cardiovasc Intervent Radiol 2009 32:514-21.
- [2] Krämer, N A. et al. Investigative Radiology 2009 44:390-7.
- [3] Tzifa, A et al *Circ Cardiovasc Interv* 2010 3:585-92.
- [4] Bieri, O. et al Magn Reson Med 2007 58:1242-8.
- [5] Patil, S, et al. Magn Reson Med 2009 62:935-42.
- [6] Chen, S et al. *J. AM. CHEM. SOC* 2010 132:15022-29.